



## Advantages and limitations of the nonlinear Schrödinger equation in describing the evolution of nonlinear water-wave groups

Lev Shemer

School of Mechanical Engineering, Tel-Aviv University, Tel-Aviv 69978, Israel; [shemer@eng.tau.ac.il](mailto:shemer@eng.tau.ac.il)

Received 13 November 2014, accepted 30 March 2015, available online 28 August 2015

**Abstract.** The nonlinear Schrödinger (NLS) equation is a popular and relatively simple model used extensively to describe the evolution of nonlinear water-wave groups. It is often applied in relation to the appearance of extremely steep (freak, or rogue) waves in the ocean. The limits of the applicability of the NLS equation, and in particular the relevance of the model to rogue waves, are examined here on the basis of quantitative and qualitative comparison with an experiment.

**Key words:** nonlinear water waves, nonlinear Schrödinger equation, breaking waves, rogue waves, breathers, Peregrine breather.

### 1. INTRODUCTION

In recent years, the nonlinear Schrödinger (NLS) equation has attracted considerable attention as a possible model for describing the evolution of wave trains in deep and intermediate-depth water. To a large extent, this interest is prompted by the existence of a special class of analytic solutions to the NLS equation, the so-called breathers. These envelope solitons are periodic in time and/or in space, and exhibit a modulation pattern in which an initially small hump in the envelope is amplified significantly due to the focusing properties of the deep-water NLS equation. This evolution pattern reminds observations of the so-called rogue, or freak, waves in the oceans. These abnormally high waves appear unexpectedly and then disappear.

Understanding the mechanisms leading to the appearance of rogue waves is important not only scientifically but also due to the potential of such extreme waves to cause extensive damage to marine and off-shore structures as well as to marine transportation. The qualitative similarities between the NLS breather solutions and rogue waves prompted suggestions that the NLS breathers can serve as a prototype of rogue waves in the ocean [1]. It was also asserted that some types of unidirectional NLS solitons, including the so-called Peregrine [2] breather (PB), were actually observed in laboratory experiments [3]. Experimental observations of PB were also reported in nonlinear fibre optics and in multi-component plasma. Following these

studies, Shemer and Alperovich [4] performed detailed measurements of the propagating PB in a medium-sized wave tank and provided evidence that both qualitative and quantitative agreement between the NLS solution and the experimental results is incomplete. In this paper, the limitations of the NLS equation are examined by carrying out comparison between the NLS simulations and the results of measurements in laboratory wave tanks. More advanced models describing evolution of nonlinear unidirectional water waves are also considered.

### 2. THEORETICAL MODELS

The variation in space  $x$  and in time  $t$  of the surface elevation  $\zeta$  in a narrow-banded deep-water wave group with the carrier frequency  $\omega_0$  and the wave number  $k_0$  can be presented at the leading order as

$$\zeta(x, t) = \text{Re}[a(x, t)e^{i(k_0x - \omega_0t)}], \quad (1)$$

where  $a(x, t)$  is the complex group envelope that is presumed to vary slowly in time and space. The frequency and the wave number satisfy the deep-water dispersion relation  $\omega_0^2 = k_0g$ . The wave steepness  $\varepsilon = a_0k_0$ , where  $a_0$  is the characteristic wave amplitude, constitutes the small parameter of the problem. It is used to define the following dimensionless scaled variables in the frame of reference moving with the group velocity  $c_g$  [4]:

$$\xi = \varepsilon\omega_0(x/c_g - t); \quad \eta = \varepsilon^2k_0x; \quad A(\xi, \eta) = a/a_0. \quad (2)$$

The NLS equation describing evolution along the tanks of the complex normalized envelope  $A(\xi, \eta)$  from the initial condition prescribed at the wavemaker located at  $\eta = 0$  has the following form:

$$-i\frac{\partial A}{\partial \eta} + \frac{\partial^2 A}{\partial \xi^2} + |A|^2 A = 0. \quad (3)$$

Dysthe [5] derived a modified, 4th order version of the NLS equation that accounts for finite spectral width and describes the evolution of the spatial distribution of the complex envelope of the narrow-banded wave train in time. The spatial evolution version of the model that is appropriate for carrying out quantitative comparison between the experimental and the theoretical results can be written as [6,7]:

$$\begin{aligned} \frac{\partial A}{\partial \eta} + i\frac{\partial^2 A}{\partial \xi^2} + i|A|^2 A + 8\varepsilon|A|^2 \frac{\partial A}{\partial \xi} + 2\varepsilon A^2 \frac{\partial A^*}{\partial \xi} \\ + 4i\varepsilon A \frac{\partial \Phi}{\partial \xi} = 0; \end{aligned} \quad (4)$$

$$4\frac{\partial^2 \Phi}{\partial \xi^2} + \frac{\partial^2 \Phi}{\partial Z^2} = 0; \quad Z < 0. \quad (5)$$

The scaled dimensionless velocity potential  $\Phi(\eta, \xi, Z)$  and the vertical coordinate  $Z$  are related to the dimensional  $\phi(x, z, t)$  and  $z$  by  $\Phi = \omega_0 a_0^2 \phi$ ,  $Z = \varepsilon k_0 z$ , respectively. The NLS Eq. (3) and the first three terms in the Dysthe model (4) that are identical to the LHS of (3), are all of the 3rd order in  $\varepsilon$ , as can be easily seen from (2). The following terms in (4) are of the 4th order, so that the equation is formally inconsistent. The order of the NLS equation reflects the fact that for deep water waves, the lowest-order non-trivial interactions occur among four waves at the 3rd order in the wave steepness  $\varepsilon$ . Zakharov [8] derived the most general equation that describes evolution of the wave field in the wave-vector Fourier space at this order and has no spectral limitations. A spatial version of the Zakharov equation [7,9] describes evolution in space of each frequency harmonic of the spectrum. It was demonstrated in [7,10] that the Dysthe model can be derived from the temporal or spatial versions of the Zakharov [8] equation. These derivations make it evident that both temporal and spatial versions of the Dysthe [5] equation are of the 3rd order in the wave steepness  $\varepsilon$ . Both those versions are obtained once it is assumed that the relative spectral width is of the order  $\varepsilon$  as well. All 4th order terms in (4) stem from accounting for the finite spectral width by taking the leading (linear) term in the Taylor expansion of the deep-water dispersion relation  $\Delta|\vec{k}|/|\vec{k}_0| = O(\varepsilon)$  for the temporal evolution or  $\Delta(\omega)/\omega_0 = O(\varepsilon)$  for the spatial evolution case. The nonlinear term in the NLS equation is obtained from (4) for vanishing spectral width.

### 3. THE PEREGRINE BREATHER

The Peregrine [2] analytic solution of (1) for the complex envelope  $A(\xi, \eta)$  has the following form:

$$A(\xi, \eta) = -\sqrt{2}\left[1 - \frac{4(1-4i\eta)}{1+4\xi^2+16\eta^2}\right]e^{-2i\eta}. \quad (6)$$

The solution (6) is symmetric with respect to the scaled dimensionless time  $\xi$ . At the origin  $|A(0,0)| = 3\sqrt{2}$ , while  $|A(\eta \rightarrow \pm\infty, \xi \rightarrow \pm\infty)| = \sqrt{2}$ , so the maximum absolute of the envelope value at  $\xi = 0; \eta = 0$  exceeds the background  $\zeta_0 = \sqrt{2}a_0$  by a factor of 3. An initially small hump in a nearly monochromatic wave train corresponding to finite values of  $|\eta|$  is thus amplified significantly as  $|\eta| \rightarrow 0$ . For that reason, PB was suggested as a major possible route to deterministic freak waves generation [1]. Experiments on PB were carried out for the following set of parameters: carrier wave amplitude  $\zeta_0 = 0.01$  m, period  $T_0 = 0.587$  s, corresponding to  $k_0 = 11.67$  m<sup>-1</sup>;  $\lambda_0 = 0.538$  m, and  $\varepsilon = a_0 k_0 = 0.0825$ . No breaking along the tank was observed. The wavemaker driving signal was calculated using (1), (2), and (6), the maximum amplitude of PB was set at the distance of 9 m from the wavemaker, corresponding to the scaled dimensional coordinate of the group was selected to be  $70T_0$ , with tapering windows over two end periods. Measurements were performed at more than 30 locations along the tank.

A summary of the experimental results of Shemer and Alperovich [4] is presented in Fig. 1. The dashed line in Fig. 1 represents the PB solution (5). The relative to the background height of the hump at the wavemaker is about 1.37, increasing to 3 at the prescribed distance of 9 m. Computations based on the Dysthe equation (4, 5) yield significantly slower and more moderate amplification; the maximum of about 2.7 is attained at a larger distance of nearly 12 m. For comparison, the highest crests and the deepest troughs recorded in every wave train at each location are also plotted in Fig. 1. As expected, these essentially nonlinear waves exhibit vertical asymmetry, with crests significantly larger than troughs, indicating that the contribution of the 2nd order bound waves to the instantaneous surface elevation cannot be neglected. It should be stressed that the normalized envelope  $A(\xi, \eta)$  is only valid at the leading order and does not contain higher order so-called 'bound' waves. Therefore, in computations of the envelope at the leading order from the experimentally determined temporal variation of the surface elevation at each measurement location, contribution of low- and high-frequency bound waves has to be eliminated.

The domains of both the low- and high-frequency 2nd order and even of the 3rd order bound waves can be clearly identified in frequency spectra of the surface elevation, see Fig. 2. The recorded signals were thus band-pass filtered in the range  $1 \text{ Hz} < f < 3 \text{ Hz}$  corresponding to the free wave domain; the envelopes

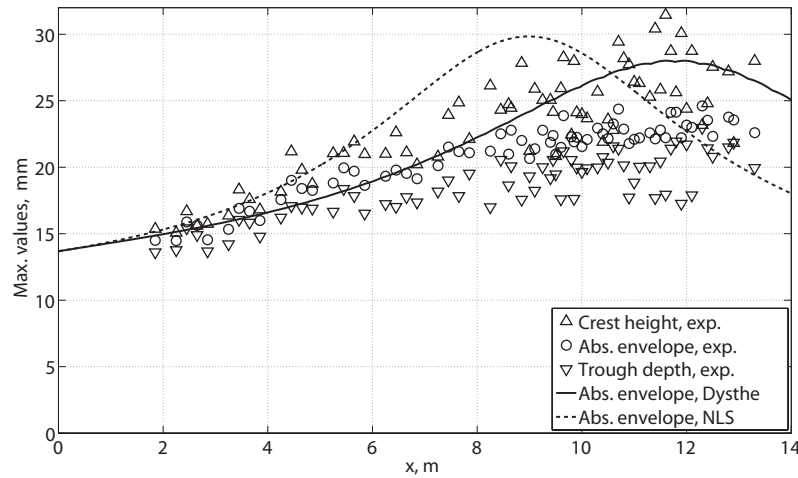


**Fig. 1.** Evolution along the tank of the extreme absolute values of the complex envelope: experiments vs computations. The measured maximum values of crests and troughs are plotted as well.

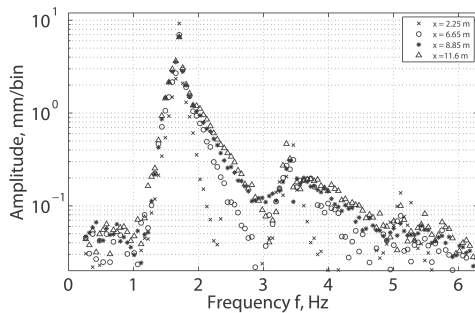


**Fig. 2.** Variation of the surface elevation spectra.

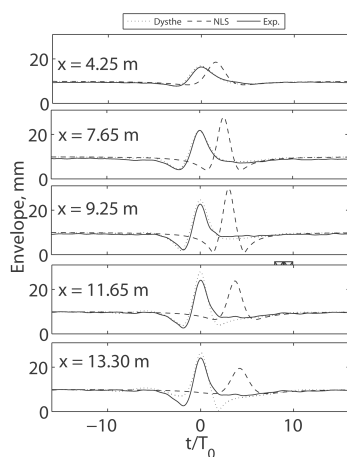


**Fig. 3.** Distribution of absolute values of the complex envelope: computations vs experiment.

of the filtered records were then computed using the Hilbert transform (for details see [11]). The variation along the tank of the maxima of the absolute values of

the resulting envelopes is presented in Fig. 1. The relative amplification of the envelope does not exceed 2.7, and is attained at about 12 m from the wavemaker, significantly farther than the prescribed by the PB soliton distance of 9 m. Figure 2 demonstrates that the initially symmetric spectra become notably asymmetric as the wave train propagates along the tank, in contrast to the behaviour of the PB spectra that retain their symmetric shape.

The absolute values of the envelopes are plotted in Fig. 3. The PB envelopes computed using (6) retain symmetry around the peak along the test section. The envelope shapes derived from the measurements, as well as those computed using the Dysthe equation (4, 5), exhibit significant asymmetry and differ notably from the PB solution; they agree well up to about  $x = 10$  m. Moreover, the velocity of propagation of the envelope in measurements and in computations based on the Dysthe equation is markedly higher than the linear group velocity as assumed in the NLS equation. The discrepancies between the experimental and numerical results based on (4, 5) increase with  $x$ . These findings demonstrate that the agreement between the analytical solution of the NLS equation given by (6) and the experiment is only maintained at the initial stages of the spatial evolution of the unidirectional wave train as long as the frequency spectrum of the surface elevation remains sufficiently narrow. Nonlinearity of the evolution process that initiates from a nearly monochromatic wave train leads to a significant widening of the frequency spectrum. Since the NLS equation is only valid for a spectrum with a vanishing width, it ceases to be applicable for the description of more advanced stages of the PB evolution. The same conclusion holds regarding other breathers, as also confirmed in a recent numerical study by Slunyaev and Shrira [12].

The Dysthe model seems to be advantageous in capturing the finer details of the wave field evolution, such as an essential left–right asymmetry of both the spectra and the envelope. All types of breathers, as well as rogue waves that were actually recorded in the ocean, exhibit fast variation of the wave train envelope (on scales comparable with the dominant wave period). They are therefore essentially wide-banded, and the emergence of a single high wave can be seen as resulting from a positive interference of numerous harmonics. In this sense, both breathers and rogue waves in the ocean (such as the well-known New Year wave) are not different from those observed by focusing on an initially wide-banded unidirectional wave train [9].

The relation between the height of the steepest wave in the train of finite duration and the shape of its discrete spectrum can be examined on the basis of simple considerations. For a given complex amplitude spectrum of the surface elevation  $a_i = a(\omega_i)$ , the crest height cannot exceed the value attained when the phases of all harmonics coincide:  $\eta_{\max} = \sum |a_i|$  (perfect coherence). For an initially nearly monochromatic wave with a narrow spectrum the energy is concentrated at the carrier wave frequency, so that  $\eta_{\max} \approx |a_{\text{carrier}}|$ . The energy conservation at the leading order requires that at any instant  $\sum a_i^2(t) \approx |a_{\text{carrier}}(t=0)|^2$ . The maximum possible wave corresponding to the sum of the amplitudes of all harmonics in the spectrum thus can be obtained when the wave energy is distributed uniformly among numerous harmonics. In this respect it can be noted that the Dirac  $\delta$ -functions that can be seen as an ultimate rogue wave have a uniform white spectrum. Therefore, in order to obtain a single extremely steep wave in the evolution process, significant spectral widening needs to occur. The rogue wave then can be seen as a result of an essentially linear constructive interference of numerous harmonics [9]. Contrary to the instantaneous surface shape that can vary fast with the change of phases of the harmonics, the spectral variations are essentially nonlinear and thus occur on slow time–space scales. It thus appears that the rogue waves constitute an inherently wide-banded phenomenon where separation of slow/fast scales is not applicable. This renders the intrinsically narrow-banded NLS equation inadequate for quantitatively accurate modelling. Nevertheless, results presented in Fig. 1 demonstrate that the maximum wave crest height of the PB may indeed be enhanced significantly, although the process of amplification differs essentially from the PB solution (6).

The question arises whether the PB and other NLS solitons constitute a special class of wave groups that are characterized by the appearance of very high wave crests in the evolution process. To answer this question, the available information on the evolution of nonlinear wave groups should be examined. Propagation along the tank of initially symmetric narrow-banded unidirectional wave groups with different initial spectra was studied experimentally by Shemer et al. [11] for deep

and intermediate-depth water. Results of the measurements were compared quantitatively with the numerical simulations based on the NLS equation. It was noticed in that study that for different wave shapes in deep water the maximum amplitudes grow initially; however, the rates of their growth are significantly below the NLS-derived predictions. In all cases both the group envelopes and the spectra develop notable left–right asymmetry. Similarly, the maximum crest heights remain lower than those in the NLS simulations. These results suggest that unidirectional wave trains with the initial conditions corresponding to various NLS breathers behave similarly to other initially narrow-banded wave groups with arbitrary shapes. In this sense it is possible to state that the NLS envelope solitons do not possess any special properties that distinguish them from non-soliton wave groups. Contrary to focusing in deep water, in experiments in shallower water with the dimensionless depth  $k_0 h < 1.36$  defocusing was observed and the maximum crest height decreased along the tank, in qualitative agreement with the NLS simulations. The results obtained in Shemer et al. [11] indicate that the NLS equation indeed captures successfully the global features of transformation along the tank of initially narrow-banded wave groups in deep and relatively shallow water. The equation also reflects in general correctly the effect of nonlinearity  $\varepsilon$  on wave field evolution; the scaling given by (2) yields the characteristic slow scales of evolution in time and space. It was thus concluded in [11] that the NLS equation may be seen as a robust, albeit crude, model for the description of wave group evolution. It also should be stressed that, in spite of the reservations concerning the applicability of the NLS equation to deep water expressed above, solitons constitute an elegant set of analytic solutions of the NLS equation that can be effectively used in laboratory experiments. The limitations on the applicability of the NLS solutions, however, certainly need to be accounted for.

As can be seen in Fig. 1, the NLS equation remains reasonably accurate at the initial stages of the wave train evolution as long as the spectrum remains sufficiently narrow. This feature was exploited recently in an experimental investigation of the wave breaking process by Shemer and Liberzon [13]. In their study, PB solution was applied to calculate the wavemaker driving signal required to generate repeatable wave breaking events at a fixed prescribed location. These conditions made it possible to demonstrate experimentally that the crest of the steepest wave slows down while growing due to nonlinear focusing, so its velocity falls notably below the wave celerity  $c_p$ . The crest slowdown process is accompanied by a notable increase in the fluid velocity at the crest of the steepest wave. The slowdown of the crest movement together with the acceleration of the fluid particles at the crest eventually result in water velocity attaining that of the crest; under these conditions inception of wave breaking is observed. The breaking thus occurs when the modified kinematic criterion for

wave breaking is satisfied. This criterion requires that breaking occurs when the liquid velocity at the wave crest attains that of the crest. It is important to stress that the crest velocity actually differs from both phase and group velocities of the wave train.

In summary, the NLS equation may be very useful in describing the general features of an evolving, initially narrow-banded, water-wave train in deep and intermediate-depth water. The focusing properties of the deep-water NLS equation, however, inevitably lead to significant spectral widening, which violates the basic assumptions adopted in the derivation of the NLS equation. For a broad spectrum that characterizes wave trains with wave energy focused in one or few steep waves, no quantitative agreement between the NLS solutions and experiments can therefore be expected. This conclusion applies to envelope solitons as well as to wave trains with an arbitrary envelope shape and an initially narrow spectrum. The NLS equation thus cannot be seen as a reliable quantitative model for studies of rogue waves in the sea.

#### ACKNOWLEDGEMENT

This study was supported in part by grant No. 2010219 from the US–Israel Binational Science Foundation.

#### REFERENCES

1. Shrira, V. I. and Geogjaev, V. V. What makes the Peregrine soliton so special as a prototype of freak waves? *J. Eng. Math.*, 2010, **67**, 11–22.
2. Peregrine, D. H. Water waves, nonlinear Schrödinger equations and their solutions. *J. Austr. Math. Soc.*, Ser. B., 1983, **25**, 16–43.
3. Chabchoub, A., Hoffmann, N. P., and Akhmediev, N. Rogue wave observation in a water wave tank. *Phys. Rev. Lett.*, 2011, **106**, 204502.
4. Shemer, L. and Alperovich, L. Peregrine breather revisited. *Phys. Fluids*, 2013, **25**, 051701.
5. Dysthe, K. B. Note on the modification of the nonlinear Schrödinger equation for application to deep water waves. *Proc. Roy. Soc. London*, 1979, **A369**, 105–114.
6. Lo, E. and Mei, C. C. A numerical study of water-wave modulation based on higher-order nonlinear Schrödinger equation. *J. Fluid Mech.*, 1985, **150**, 395–416.
7. Kit, E. and Shemer, L. Spatial versions of the Zakharov and Dysthe evolution equations for deep-water gravity waves. *J. Fluid Mech.*, 2002, **450**, 201–205.
8. Zakharov, E. Stability of periodic waves of finite amplitude on a surface of deep fluid. *J. Appl. Mech. Tech. Phys.*, (English transl.), 1968, **2**, 190–194.
9. Shemer, L., Goulitski, K., and Kit, E. Evolution of wide-spectrum unidirectional wave groups in a tank: an experimental and numerical study. *Eur. J. Mech. B/Fluids*, 2007, **26**, 193–219.
10. Stiassnie, M. Note on the modified Schrödinger equation for deep water waves. *Wave Motion*, 1984, **6**, 431–433.
11. Shemer, L., Kit, E., Jiao, H., and Eitan, O. Experiments on nonlinear wave groups in intermediate water depth. *J. Waterway, Port, Coastal & Ocean Engineering*, 1998, **124**, 320–327.
12. Slunyaev, V. V. and Shrira, V. I. On the highest non-breaking wave in a group: fully nonlinear water wave breathers versus weakly nonlinear theory. *J. Fluid Mech.*, 2013, **735**, 203–248.
13. Shemer, L. and Liberzon, D. Lagrangian kinematics of steep waves up to the inception of a spilling breaker. *Phys. Fluids*, 2014, **26**, 016601.

## Mittelineaarse Schrödingeri võrrandi eelised ja piirangud mittelineaarsete pinnalainete rühmade kirjeldamisel

Lev Shemer

Mittelineaarne Schrödingeri võrrand on populaarne ja tehniliselt realistlik võimalus suhteliselt laugete mittelineaarsete pinnalainete rühmade kirjeldamiseks. Sageli rakendatakse seda võrrandit aga piiripealsetes olukordades väga järskude struktuuride analüüsimiseks. Töös on vaadeldud mittelineaarse Schrödingeri võrrandi sobivust hiidlainete kirjeldamiseks teoreetiliste ja eksperimentaalsete tulemuste kvantitatiivse ning kvalitatiivse võrdluse kaudu. On näidatud, et kõnesolev võrrand üldiselt ei reprodutseeri hiidlainete kvantitatiivseid omadusi.